

PG02

フォトクロミック法による液柱マランゴニ対流の表面流速
測定—深層学習による宇宙実験データの再解析

Surface Velocity Measurement of Marangoni Convection in a Liquid bridge using Photochromic Dye Activation Method—Reanalysis of Data from Space Experiment by Deep Learning

矢野大志¹, 中西裕二¹, 西野耕一²

Taishi YANO¹, Yuji NAKANISHI² and Koichi NISHINO²

¹神奈川大学, Kanagawa University

²横浜国立大学, Yokohama National University

1. Introduction

It has been more than 15 years since the first series of Marangoni Experiment in Space (MEIS, hereinafter) was carried out aboard the International Space Station (ISS, hereinafter)^{1,2}. This space experiment is widely known as the first Marangoni-convection experiment on the ISS as well as the first science mission in the Kibo Japanese Experiment Module. Marangoni convection (or thermocapillary convection) in a liquid bridge, shown in **Figure 1(a)**, is the flow driven by the surface tension difference, which is caused by the temperature gradient along the free surface. One of the most important features of this fluid phenomenon is the hydrodynamical or hydrothermal-wave instability. As demonstrated by many previous studies³⁻⁵, Marangoni convection in liquid bridges transitions from an axisymmetric steady state to either a non-axisymmetric oscillatory state due to hydrothermal-wave instability (in the case of high Prandtl numbers) or a non-axisymmetric steady state due to hydrodynamical instability (in the case of low Prandtl numbers) as the driving force of convection increases. Our space experiment MEIS focused on the former instability and aimed to determine the transition conditions of the flow regime (i.e., steady or oscillatory) of Marangoni convection in a liquid bridge of high-Prandtl-number fluid under a wide variety of experimental condition. Additionally, it measured the flow and temperature fields to understand the spatiotemporal structure of both steady and oscillatory Marangoni convection.

All the experiments were performed in the Fluid Physics Experiment Facility (FPEF, hereinafter) mounted on the Kibo module. This facility was equipped with various instruments such as the particle tracking velocimetry (PTV, hereinafter)^{6,7} and the photochromic dye activation (PDA, hereinafter) method^{1,8}. These measurement techniques greatly contributed to the success of the space experiments, with the former being primarily used to measure the internal bulk flow and the latter being primarily used to measure the surface flow. However, there are somewhat fewer reports on the results of the PDA method compared to those of

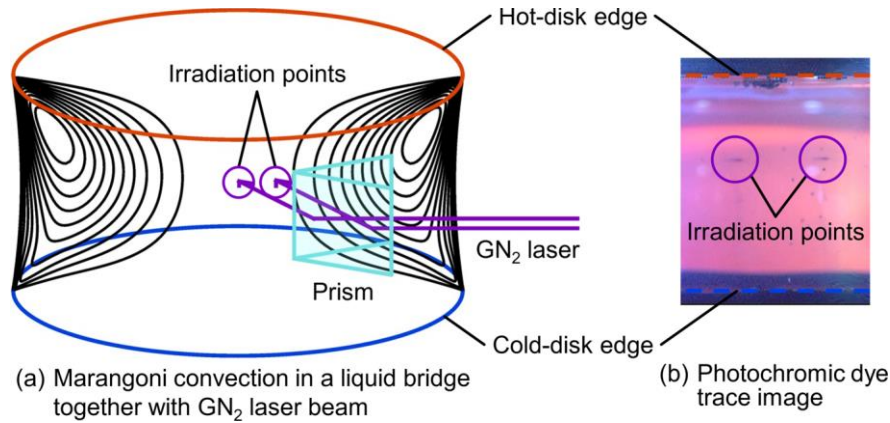


Figure 1. (a) Schematic diagram of Marangoni convection in a liquid bridge together with gaseous nitrogen laser beam for photochromic dye activation method and (b) photochromic dye trace image obtained in the space experiment.

PTV due to the following reasons: (1) PTV was performed in all series of MEIS, whereas PDA method was employed in a limited number of series; (2) there are difficulties in the automatic analysis of data acquired by the PDA method in MEIS; (3) a shortage of analysis personnel. This study aims to revisit the data of PDA method obtained in past MEIS experiments through a new data analysis method, namely deep learning with the convolution neural network (CNN, hereinafter).

2. Photochromic dye activation (PDA) method

The PDA method is one of the molecular tagging velocimetry techniques originally developed by Popovich and Hummel⁹⁾. In this method, the photochromic dye is dissolved in the working liquid, and the excitation light, such as a pulsed ultraviolet laser, is irradiated at the point where the velocity is to be measured. The photochromic dye irradiated by the excitation light changes color, and the flow velocity can be obtained by tracking the movement of the colored region. Since the activated dye returns to its original color within a short period (typically several seconds), the measurement can be repeated. Since the PDA method is a contactless velocimetry technique suitable for measuring the flow velocity near a wall or a liquid-gas interface, it has sometimes been used to measure the surface velocity of Marangoni convection in a liquid bridge^{10,11)}.

Surface velocity measurements using the PDA method were performed in the second and the third series of MEIS (i.e., MEIS-2 and MEIS-3, respectively) out of a total of five series. The diameter of the supporting disks was 30 mm for both series. Silicone oils with the typical kinematic viscosities of 5 and 20 cSt, resulting in Prandtl numbers of $Pr = 67$ and 207, were used as the working liquids. The photochromic dye TNSB¹¹⁻¹³⁾—1,3,3-trimethyl-6'-nitrospiro[indoline-2,2'-chromene]—was dissolved in silicone oils at a concentration of 0.05% by weight, and a pulsed gaseous nitrogen (GN_2 , hereinafter) laser beam with a wavelength of 337.1 nm and a pulse energy of 300 J was used to activate it. As shown in **Figure 1(a)**, the GN_2 laser beam was split into two, reflected by a prism, and irradiated two spots on the liquid-bridge surface at the same axial position but different azimuthal positions. **Figure 1(b)** shows an image captured by a CCD camera for the PDA method, obtained during MEIS-2, and referred to hereinafter as a photochromic image. As can be seen from this image, the irradiated regions appear dark pink or purple against a light pink background. The surface velocity can be measured by tracking these colored regions; however, there is an issue because the tracer particles for the PTV also appear purple, similar to the photochromic dye traces. In the previous studies^{1,8)}, activated

photochromic dyes and tracer particles were distinguished manually. However, such manual operations require an enormous amount of time for data analysis. Therefore, in this study, the process was automated (actually semi-automated) using deep learning with CNN. The details of the analysis procedure are described in the next section.

3. Deep learning Photochromic dye activation (PDA) method

Before using deep learning, it is necessary to detect candidates of activated photochromic dye on the image. In the previous studies^{1,8)}, the analysis region was limited to the vicinity of the laser beam irradiation points, and activated photochromic dyes were detected only based on brightness levels. In contrast, this study employs the following morphological image processing: (1) invert image colors; (2) create a background by averaging a time series of inverted images; (3) subtract the background from the inverted images; (4) binarize the subtracted images with an appropriate threshold; (5) fill holes (i.e., small black regions); (6) remove connected objects (pixels) smaller than a specified area; (7) computes the Euclidean distance transform; (8) suppress regional minima using the H-minima transform; (9) separate clustered objects by watershed transform. **Figures 2(a)** and **2(b)** show the original photochromic image and the background-subtracted photochromic image, respectively. In **Figure 2(b)**, purple rectangles indicate objects detected by the above operations. Through morphological image processing, purple (or dark pink) objects can be detected automatically not only in the vicinity of the laser beam irradiation points but also in the entire photochromic image. Additionally, it becomes possible to detect photochromic dye traces whose color is returning to the original after some time has elapsed since the color change. However, it follows from **Figure 2** that other objects, such as tracer particles and noise, are also detected in addition to the activated photochromic dye traces. In order to classify these detected objects into *photochromic dyes*, *tracer particles*, and *others*, deep learning with CNN is used.

The architecture of the CNN used for classification is shown in **Figure 3**. This network is designed based on the VGGNet¹⁴⁾ proposed by the Visual Geometry Group at the University of Oxford, which consists of many convolutional layers with small filter sizes. The input to this CNN is volume data consisting of five layers. The first three layers represent the red, green, and blue components of an image with a size of 49×51 pixels, cropped around the objects detected with the aforementioned morphology image processing. The last two

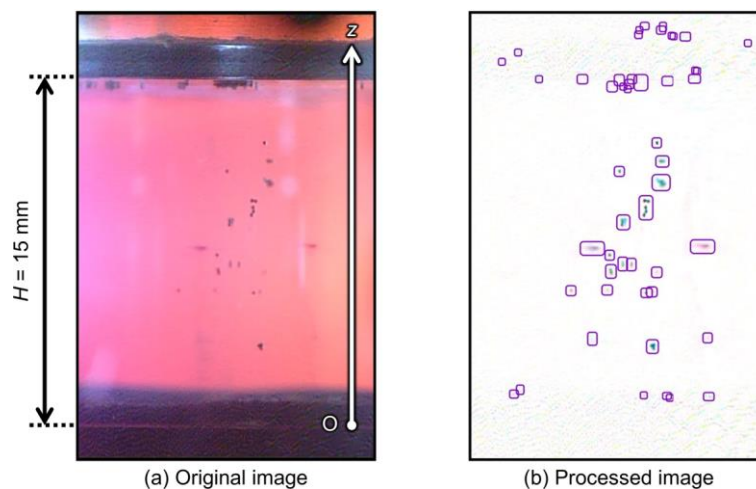


Figure 2. (a) Original and (b) background subtracted and brightness adjusted photochromic dye trace images. Purple rectangles in (b) indicate objects detected by the morphological image processing.

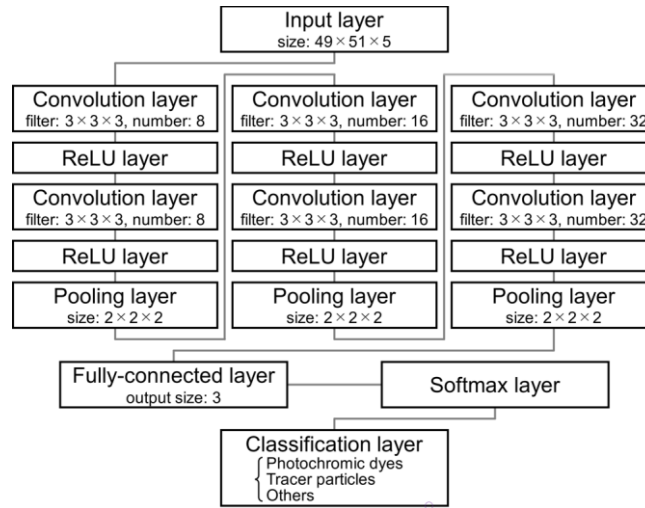


Figure 3. Architecture of the convolution neural network for classifying the detected objects into *photochromic dyes*, *tracer particles*, and *others*.

layers represent the vertical and horizontal positions of each pixel on the photochromic image. **Figures 4(a)–4(c)** show visualizations of input data for *photochromic dyes*, *tracer particles*, and *others*. If the CNN is sufficiently optimized, it will output correct classification results for the inputs. In order to optimize the CNN (or to determine the weighting coefficients and biases for each layer), it is necessary to prepare a large set of training data, as shown in **Figure 4**. In this study, 300 training data are manually prepared for each category—*photochromic dyes*, *tracer particles*, and *others*—totaling 900 training data. Such manual operations are only performed at the beginning, with subsequent analysis conducted automatically; therefore, it is described as “actually semi-automated” in the previous section. **Figure 5** shows the training history for each iteration, wherein the red line indicates the accuracy of classification (see left vertical axis), and the green line indicates the cross-entropy loss (i.e., the indicator of the CNN’s poor performance, see right vertical axis). The algorithm known as stochastic gradient descent with momentum¹⁵⁾ is used to optimize the CNN, with the batch size and the maximum number of epochs set to 15 and 100, respectively. The initial learning rate is set to 1×10^{-5} and is updated (decreased) periodically. Through iterative computation, the classification accuracy increases to nearly 100%, while the cross-entropy loss significantly decreases. These results indicate that the CNN used in this study is well-optimized for the training data. In the subsequent data analysis, the objects detected by morphological image processing are classified into three categories (i.e., *photochromic dyes*, *tracer particles*, and *others*), and the surface velocity is obtained by tracking those classified as *photochromic dye*.

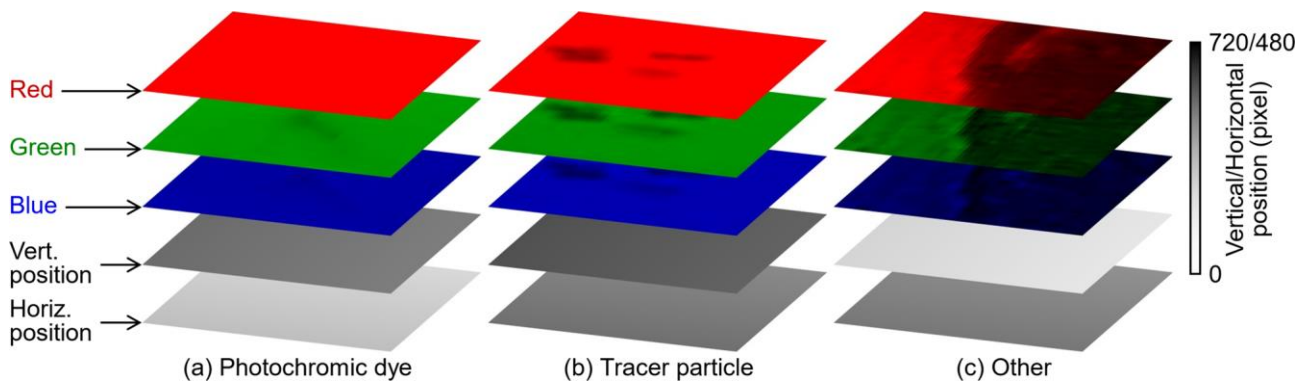


Figure 4. Examples of training data used for optimizing the convolution neural network: (a) *photochromic dyes*, (b) *tracer particles*, and (c) *others*.

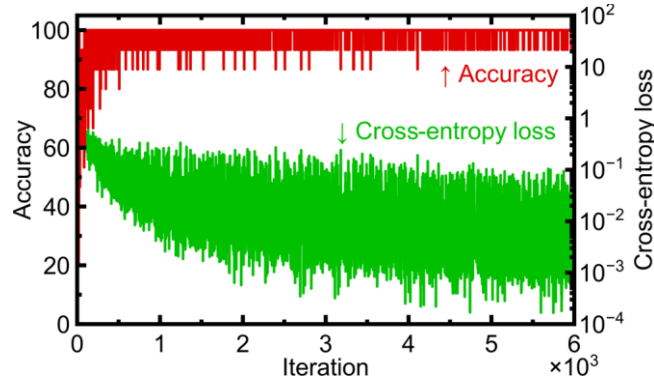


Figure 5. Training history of convolutional neural network: classification accuracy (red line, see left vertical axis) and cross-entropy loss (green line, see right vertical axis).

4. Surface velocity of steady Marangoni convection

The surface velocity of Marangoni convection in a liquid bridge observed in MEIS-2 is measured using a newly developed method. The experimental conditions considered here are as follows: the liquid bridge height is $H = 15$ mm, and the temperature difference between the supporting disks is $\Delta T = 5.7$ K, which results in steady Marangoni convection because this ΔT is sufficiently lower than the instability threshold (i.e., 7.5 K). The axial component u_z of the surface velocity measured with the present method is plotted as a function of the axial position z in **Figure 6**, along with those evaluated using the previous method^{1,8)} and the numerical simulation^{1,8)}. In the FPEF, the measurement position of the PDA method could be changed by moving the laser beam irradiation points along the z direction. However, in the corresponding experiment, the laser beam irradiation positions were limited to four points due to time limitations, and therefore, the previous PDA method could only measure the velocity at these specific locations. As shown in **Figure 6**, the newly developed method can detect photochrome dye traces that have moved downstream and improves spatial resolution in the z direction. The magnitude of u_z tends to be slightly larger than the previous measurement and the numerical simulation. However, the obtained surface velocities are reasonably consistent each other and show the well-known tendency that the magnitude of the surface velocity increases with approaching the warmer side, except in the very vicinity of the disk. Additionally, it is confirmed that the azimuthal velocity converges to zero, which is characteristic of steady Marangoni convection. These results demonstrate that the data analysis developed in this study is effective for application to the PDA method in MEIS.

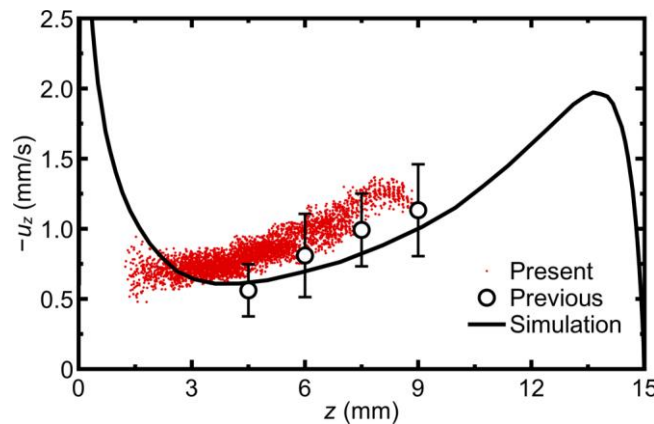


Figure 6. Axial distributions of the negative z -direction component of the surface velocity obtained by present method (red dots), previous method (white circles), and numerical simulation (black line).

5. Summary

This study aims to develop a new data analysis technique for the photochromic dye activation method in space experiments on Marangoni convection in a high-Prandtl-number liquid bridge. To achieve this goal, object detection using morphology image processing and data classification using deep learning with convolutional neural network are employed. The developed method is applied to the data obtained from the past space experiment (i.e., MEIS-2), and the surface velocity of axisymmetric steady Marangoni convection is measured. The newly developed method provides reasonable results and improves spatial resolution in the axial direction of the liquid bridge. This method is expected to analyze previously untouched data from space experiments and enhance understanding of Marangoni convection in a liquid bridge of high-Prandtl-number fluid.

References

- 1) H. Kawamura, K. Nishino, S. Matsumoto and I. Ueno: Report on microgravity experiments of Marangoni convection aboard International Space Station. *J. Heat Transfer*, **134** (2012) 031005, DOI: [10.1115/1.4005145](https://doi.org/10.1115/1.4005145).
- 2) K. Nishino, T. Yano, H. Kawamura, S. Matsumoto, I. Ueno and M.K. Ermakov: Instability of thermocapillary convection in long liquid bridges of high Prandtl number fluids in microgravity. *J. Cryst. Growth*, **420** (2015) 57, DOI: [10.1016/j.jcrysgro.2015.01.039](https://doi.org/10.1016/j.jcrysgro.2015.01.039).
- 3) D. Schwabe, A. Scharmann, F. Preisser and R. Oeder: Experiments on surface tension driven flow in floating zone melting. *J. Cryst. Growth*, **43** (1979) 305, DOI: [10.1016/0022-0248\(78\)90387-1](https://doi.org/10.1016/0022-0248(78)90387-1).
- 4) M. Wanschura, V.M. Shevtsova, H.C. Kuhlmann and H.J. Rath: Convective instability mechanisms in thermocapillary liquid bridges. *Phys. Fluids*, **7** (1995) 912, DOI: [10.1063/1.868567](https://doi.org/10.1063/1.868567).
- 5) H.C. Kuhlmann: *Thermocapillary Convection in Models of Crystal Growth*, Springer-Verlag Berlin Heidelberg (1999), DOI: [10.1007/BFb0109562](https://doi.org/10.1007/BFb0109562).
- 6) T. Yano, K. Nishino, H. Kawamura, I. Ueno, S. Matsumoto, M. Ohnishi and M. Sakurai: 3-D PTV measurement of Marangoni convection in liquid bridge in space experiment. *Exp. Fluids*, **53** (2012) 9, DOI: [10.1007/s00348-011-1136-9](https://doi.org/10.1007/s00348-011-1136-9).
- 7) T. Yano and K. Nishino: Flow visualization of axisymmetric steady Marangoni convection in high-Prandtl-number liquid bridges in microgravity. *Int. J. Microgravity Sci. Appl.*, **36** (2019) 360202, DOI: [10.15011/jasma.36.2.360202](https://doi.org/10.15011/jasma.36.2.360202).
- 8) S. Matsumoto, K. Nishino, I. Ueno, T. Yano and H. Kawamura: Marangoni Experiment in Space. *Int. J. Microgravity Sci. Appl.*, **31** (2014) S51.
- 9) A.T. Popovich and R.L. Hummel: A new method for non-disturbing turbulent flow measurements very close to a wall. *Chem. Eng. Sci.*, **22** (1967) 21, DOI: [10.1016/0009-2509\(67\)80100-3](https://doi.org/10.1016/0009-2509(67)80100-3).
- 10) K. Nishino: A review of the Marangoni convection experiment in TR-IA #6. *J. Jpn. Soc. Microgravity Appl.*, **20** (2003) 232: DOI: [10.15011/jasma.20.3.232](https://doi.org/10.15011/jasma.20.3.232).
- 11) S. Simic-Stefani, M. Kawaji and S. Yoda: Onset of oscillatory thermocapillary convection in acetone liquid bridges: The effect of evaporation. *Int. J. Heat Mass Transf.*, **49** (2006) 17, DOI: [10.1016/j.ijheatmasstransfer.2006.01.042](https://doi.org/10.1016/j.ijheatmasstransfer.2006.01.042).
- 12) M. Kawaji, W. Ahmad, J.M. DeJesus, B. Sutharshan, C. Lorencez and M. Ojha: Flow visualization of two-phase flows using photochromic dye activation method. *Nucl. Eng. Des.*, **141** (1993) 343, DOI: [10.1016/0029-5493\(93\)90111-L](https://doi.org/10.1016/0029-5493(93)90111-L).
- 13) M. Kawaji: Two-phase flow measurements using a photochromic dye activation technique. *Nucl. Eng. Des.*, **184** (1998) 379, DOI: [10.1016/S0029-5493\(98\)00210-6](https://doi.org/10.1016/S0029-5493(98)00210-6).
- 14) K. Simonyan and A. Zisserman: Very deep convolutional neural networks for large-scale image recognition. *arXiv preprint arXiv:1409.1556* (2014) 1, DOI: [10.48550/arXiv.1409.1556](https://doi.org/10.48550/arXiv.1409.1556).
- 15) Y. Liu, Y. Gao and W. Yin: An improved analysis of stochastic gradient descent with momentum. *Adv. Neural Inf. Proces. Syst.*, **33** (2020) 18261.



© 2024 by the authors. Submitted for possible open access publication under the terms and conditions of the Creative Commons Attribution (CC BY) license (<http://creativecommons.org/licenses/by/4.0/>).